

# Influence of composition variation on structural, magnetic and dielectric properties of $Gd_3Fe_5O_{12}(x)/MgFe_2O_4(1-x)$ composite

A Sharma<sup>1</sup>, S K Godara<sup>2</sup> and A K Srivastava<sup>1\*</sup>

<sup>1</sup>Department of Physics, Lovely Professional University, Phagwara, Punjab 144411, India

<sup>2</sup>Department of Chemistry, Guru Nanak Dev University, Amritsar, Punjab 143005, India

Received: 21 September 2021 / Accepted: 05 April 2022 / Published online: 24 May 2022

**Abstract:** Sol–gel auto-combustion method was used to prepare  $Gd_3Fe_5O_{12}$  and  $MgFe_2O_4$ . Mechanical blending was used to form the composites of  $Gd_3Fe_5O_{12}(x)-MgFe_2O_4(1-x)$  ( $x = 1.0, 0.5, 0.75$  in wt.%). X-ray diffraction (XRD) study reveals the pure phase formation of  $Gd_3Fe_5O_{12}$  and  $MgFe_2O_4$  and the presence of both phases in composites. The average crystallite size lies in the range of 26–56 nm. Field emission scanning electron microscope (FESEM) study reveals that the grains of  $Gd_3Fe_5O_{12}$  have a spherical morphology and its composites show agglomeration due to presence of magnetic interaction between ferrites nanoparticles. The dielectric study reveals that the real and imaginary parts of complex permittivity of the composites vary with the change in the composition of  $Gd_3Fe_5O_{12}$  and  $MgFe_2O_4$ . For  $x = 0.5$ , the low dielectric tangent loss ( $\tan\delta$ )  $\sim 0.35$  with high dielectric constant ( $\epsilon'$ )  $\sim 612$  was obtained at 1 MHz frequency. This suggests the use of these composites for dielectric substrate antennas. Further, the magnetic property reveals that the magnetic parameter of  $Gd_3Fe_5O_{12}$  composites varies by addition of  $MgFe_2O_4$ , i.e. at  $x = 0.5$  and  $0.75$ . The values of microwave operating frequency ( $\omega_m$ ) are 3.5 GHz and 2.5 GHz for  $x = 0.5$  and  $x = 0.75$ , respectively. These values suggest that the composites can be used in S-band.

**Keywords:** Garnet ferrite; Spinel ferrite; Sol–gel auto-combustion; Composite, Dielectric loss

## 1. Introduction

The word ferrites are now becoming a brand for many researchers and industrialist, because of its never-ending applications [1, 2]. Ferrites are ceramic oxides. Rather than ferrites, other oxides like ferroelectric metal oxides are used in electric and optical devices as they have good ferroelectric and opto-electrical properties [3]. Transition metal oxides have application in energy storage devices and sensor [4]. But due to good insulating and magnetic properties [5], a large number of researches are still going on complex oxides based on iron. Ferrites have very good insulating and magnetic properties so they are used in many devices like isolators, antennas, switches, filters, magnetic sensors, transformer core, drug carriers, memory devices, filters, microwave absorption, humidity gas sensor, and many more applications [6–11]. The properties of these ferrites are strongly dependent on the microstructure,

materials, formation methods, and type of compositions. The advanced functioning composites having controlled magnetic and dielectric property are the challenge for modern physics. Materials showing low loss with good application in the high-frequency range can provide a better option for many communication-based devices.

The ferrites are ferromagnetic materials and are divided into two categories based on their crystal structure—hexagonal (for example hexaferrites) and cubic (for examples spinel and garnet ferrites). Each ferrite has its individual properties. Hexaferrites possess very good magnetic properties and have a higher value of imaginary part of complex permittivity which provides higher losses in the material [12], but many devices require low losses with good magnetic properties where hexaferrites are of no use. Garnet ferrite is soft ferrite that easily gets magnetized and demagnetized [13, 14]. The general formula of garnet ferrite is  $R_3Fe_5O_{12}$ , where R is rare earth having three sites. The cation of rare earth  $\{R^{+3}\}$  is present in dodecahedral site 24c, whereas both 16a octahedral and 24d tetrahedral sites are occupied by iron ions  $[Fe^{+3}]$ ,  $(Fe^{+3})$ , respectively.

\*Corresponding author, E-mail: srivastava\_phy@yahoo.co.in

Good magnetic, electromagnetic, dielectric, magneto-optical, and thermal properties along with low magnetic and dielectric losses are present in garnet ferrites [15–19], which make garnet ferrite suitable for many applications like electronics, communication devices, etc. [20]. Spinel ferrites are also soft ferrite with the general formula  $MFe_2O_4$ , where M represents divalent ions like  $Fe^{+2}$ ,  $Mg^{+2}$ ,  $Mn^{+2}$ ,  $Ni^{+2}$ , or  $Co^{+2}$ . Spinel ferrite has good magnetic, dielectric property with very less value of imaginary part of complex permittivity at higher frequency, i.e. losses are very low in these ferrites [21].

Nanocomposites of these ferrites are a better option to modify their individual existing properties. The addition of these ferrites in the form of composites having distinct phases forms exchange bias as a result of which superparamagnetic limit rises, which is a very crucial parameter for device miniaturization [22, 23]. Also, the mixing of these ferrites enhances the energy product ( $BH_{max}$ ) value, which is deciding parameter for the magnet quality [24]. A large number of researchers have investigated the composites of hexaferrites with spinel ferrites and modified the dielectric and magnetic properties which targets different applications [25, 26, 28]. Algarou et al., [3] have studied the hard/soft  $SrTb_{0.01}Tm_{0.01}Fe_{11.98}O_{19}/AFe_2O_4$  composites and found that the prepared composites show good magnetic exchange coupling. Kotnala et al., [29] have worked on hard/soft mixed composites and observed that the dielectric losses decrease and coercivity increases with an increase in hard ferrite in the composites. Almessiere et al., [30] have studied  $SrFe_{12-x}V_xO_{19}/(Ni_{0.5}Mn_{0.5}Fe_2O_4)_y$  the hard/soft ferrite composites and found that the structural and magnetic properties got influenced by changing hard/soft compositions. Trukhanov et al. [31] have studied the microwave properties of the hard/soft composites of  $SrTb_{0.01}Tm_{0.01}Fe_{11.98}O_{19}-AFe_2O_4$  and found that materials are good candidate of microwave absorption. Algarou et al. [32] have studied  $SrTb_{0.01}Tm_{0.01}Fe_{11.98}O_{19}/(CoFe_2O_4)_x$  composites and found that with an increase in soft ferrite, the magnetic parameters also increase which makes these composites useful for nanomagnets.

To the best of our knowledge, no work has been done yet on the nanocomposites of garnet ferrite with spinel ferrite, i.e. on soft–soft ferrites composites. In this work, we have prepared composites of soft ferrites by wt% method to find out the effect of magnesium ferrite (spinel ferrite) on gadolinium iron garnet (garnet ferrite) on its structural, magnetic, and dielectric properties. The aim of proposed work is to explore a new composite that will yield enhanced magnetic and dielectric properties for different applications.

## 2. Experimental details

Gadolinium iron garnet ( $Gd_3Fe_5O_{12}$ ) and magnesium ferrite ( $MgFe_2O_4$ ) were prepared using the sol–gel auto-combustion method separately. For the preparation of  $Gd_3Fe_5O_{12}$  (GdIG), gadolinium (III) nitrate [ $Gd(NO_3)_3 \cdot 6H_2O$ ], ferric (III) nitrate [ $Fe(NO_3)_3 \cdot 9H_2O$ ], and citric acid ( $C_6H_8O_7 \cdot H_2O$ ) of Sigma-Aldrich and LOBA company with AR grade were used as precursors. For the preparation of  $MgFe_2O_4$ , magnesium (II) nitrate [ $Mg(NO_3)_2 \cdot 6H_2O$ ], ferric (III) nitrate [ $Fe(NO_3)_3 \cdot 9H_2O$ ], and citric acid ( $C_6H_8O_7 \cdot H_2O$ ) of LOBA company with AR grade were used as precursors. According to stoichiometric, these salts of metals were added in 100 ml of distilled water by using different beakers for the preparation of GdIG and MF and kept for stirring for half an hour on a magnetic stirrer in order to dissolve these salts in distilled water properly. After that pH of the solution was made 7 by adding ammonia solution dropwise. Then, the solutions were kept for stirring and heated at 70 °C until the solution reduces and the gel was obtained. The gel of both the solutions was heated at 200–250 °C for an hour. The gel starts drying up, swelling up and burning in presence of air. Finally, the powder was obtained. The sintering of GdIG was done at 1200 °C for 6 h in a muffle furnace. The sintering of the MF was done at 900 °C for 6 h in a muffle furnace. The sintered samples were ground using mortar pastel for half an hour to obtain a fine powder. Finally, the obtained samples were used to form composites. The GdIG sample was divided into three parts in order to make composites with MF. The composites were formed according to wt% using the equation  $mx = m(1 - x)$  where x is weight per cent, m is the total weight of material used to prepare composites.

The weighted sample were then mixed together by mechanical blending for 45 min to prepare composites with wt.% x = 1.0 (GdIG), 0.5 (GdIG 50% and MF 50%) and 0.7 (GdIG 75% and MF 25%).

X-ray diffraction (XRD) spectroscopy was used to study the phase formation and structural properties of  $GdIG(x)-MF(1-x)$  composites along with phase formation of individual soft garnet ferrite and soft spinel ferrite using a step size of 0.02 and value of  $2\theta$  in 20–80-degree range. Field emission scanning microscope (FESEM) with energy-dispersive X-ray (EDX) was used to study the morphology and chemical compositions of GdIG and its composites. An impedance analyser was used to study the dielectric properties of the GdIG and its composites. For the study of the dielectric property, circular disc-like pellets were formed and further silver paste was applied on both sides of the pellets. Vibrating sample magnetometer (VSM) was used to study the magnetic properties of GdIG and its composites.

### 3. Results and discussion

#### 3.1. XRD analysis

The XRD patterns of garnet ferrite ( $\text{Gd}_3\text{Fe}_5\text{O}_{12}$ ) and spinel ferrites ( $\text{MgFe}_2\text{O}_4$ ) are shown in Fig. 1. From the XRD pattern of both gadolinium garnet ferrite (GdIG) and magnesium spinel ferrites (MF), it has been clear that the single-phase is formed, which was confirmed from the JCPDS no. 720141 for GdIG and 711,232 for MF. A little amount of secondary phase (JCPDS no. 47-0067) has been observed in the samples. Figure 1 also represents the XRD pattern of composites of  $\text{GdIG}(x)/\text{MF}(1-x)$  with  $x$  (wt.%) 1 (Pure garnet ferrite), 0.5 and 0.75. It has been observed from the pattern that at  $x = 0.5$ , both garnet and spinel phases are present with sharper peaks corresponding to hkl values of (420) and (311), respectively. This ensures that two independent phases of both ferrites exist in the composite without any chemical reaction [29]. But by a further increase in the amount of GdIG in composites that is at  $x = 0.75$ , many peaks of MF got surpassed, and the intensity of the peaks also decreases. The intensity and number of peaks formed in XRD are dependent on the number of corresponding phases present in the sample [33].

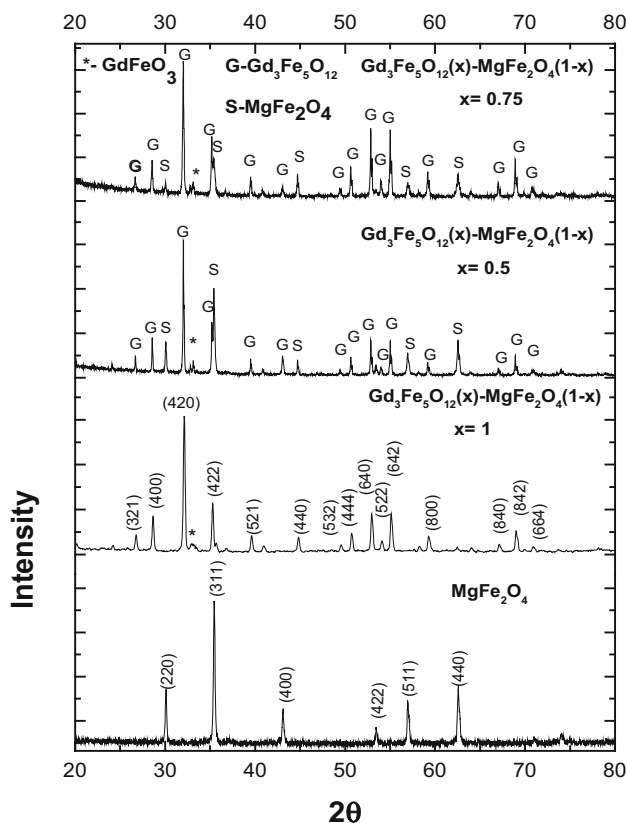


Fig. 1 XRD spectra of  $\text{MgFe}_2\text{O}_4$ ,  $(\text{Gd}_3\text{Fe}_5\text{O}_{12})_x$   $x = 1.0$ ,  $x = 0.5$ ,  $x = 0.75$

This decrease in intensity of the characteristic peak of MF implies that MF starts absorbing on the surface of GdIG and also indicates that the adhesion force between both ferrites at  $x = 0.75$  is very strong. Figure 2 represents the refined XRD pattern of the samples done by using Rietveld Refinement.

Table 1 represents the values of crystallite size, lattice constant, micro-strain, of pure GdIG, i.e.  $x = 1.0$ , MF and  $\text{GdIG}(x)/\text{MF}(1-x)$  composites at  $x = 0.5$  and  $0.75$ . The average crystallite size of the composites was calculated by using Scherrer Eq. 1.

$$D = \frac{K\lambda}{\beta \cos \theta} \quad (1)$$

Here,  $D$  is crystallite size,  $K$  is Scherrer constant with value 0.9,  $\lambda$  is the wavelength of X-ray sources with value 0.15406 nm, and  $\beta$  is full-width half maxima (FWHM) (in radians). The value of  $\beta$  was calculated from given XRD data using origin software, where  $\theta$  is the peak position (radians) and its value was also calculated from given XRD data using origin software. It has been seen that the average crystallite size of composites was found to be in the range of 33 -55 nm. The average crystallite size of GdIG composite first increases from  $x = 1.0$  to  $x = 0.5$  and then decreases at  $x = 0.75$ . At  $x = 0.5$ , both GdIG and MF are present in equal quantity and the increase in crystallite size reveals that MF is contributing towards the change in crystallite size of GdIG. Further decrease in crystallite size at  $x = 0.75$  is due to the dominance of GdIG on MF. Here, MF present in lesser amount. Also, a decrease in crystallite size at  $x = 0.75$  can be correlated with peak broadening [34] which can be clearly seen from Fig. 1. The average crystallite size of the Pure GdIG ( $x = 1$ ) is least and that for composite  $x = 0.5$  (50% GdIG and 50% MF) is largest due to nanocomposites [35]. Reason for the lesser value of crystallite size at  $x = 1\%$  is that  $D$  is inversely proportional to  $\beta$  and  $2\theta$  and it has been found that the value of  $2\theta$  for  $x = 1\%$  is largest which implies that the value of  $D$  is small.

As the structure of both garnet ferrite and spinel ferrite is cubic, so lattice constant for the composites was calculated using Eq. 2.

$$\frac{1}{d^2} = \frac{h^2 + k^2 + l^2}{a^2} \quad (2)$$

Here,  $a$  is lattice constant, hkl are the miller indices which is taken corresponded to maximum intensity peak, and  $d$  is interplanar spacing calculated by using Bragg's law (Eq. 3).

$$d_{\text{spacing}} (\text{\AA}) = \frac{n\lambda}{2 \sin \theta}, n = 1 \quad (3)$$

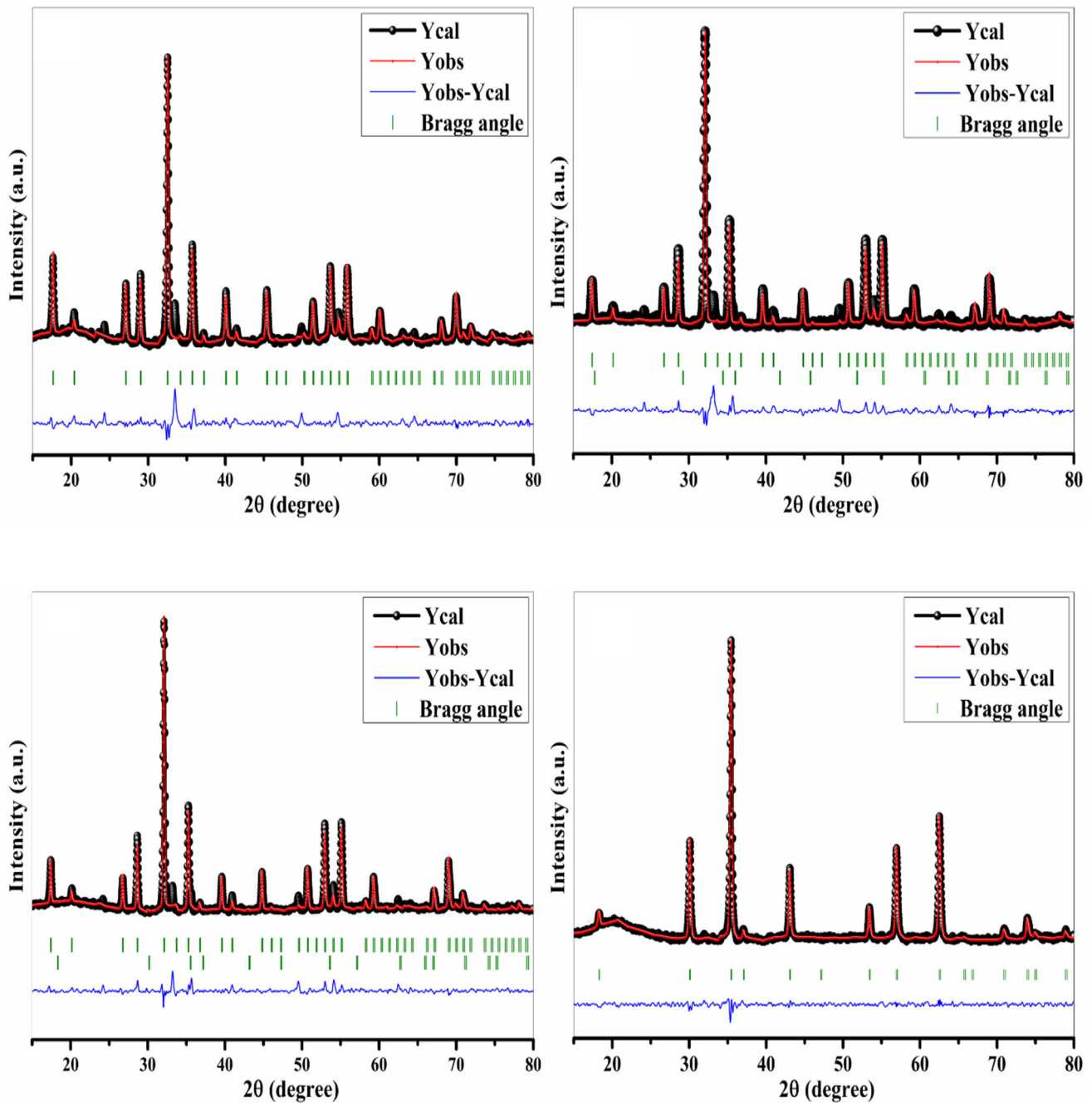


**Fig. 2** Refined XRD patterns of prepared samples (a)  $\text{Gd}_3\text{Fe}_5\text{O}_{12}$ , (b)  $(\text{Gd}_3\text{Fe}_5\text{O}_{12})_{0.5}/(\text{MgFe}_2\text{O}_4)_{0.5}$ , (c)  $(\text{Gd}_3\text{Fe}_5\text{O}_{12})_{0.75}/(\text{MgFe}_2\text{O}_4)_{0.25}$ , and (d)  $\text{MgFe}_2\text{O}_4$

The lattice constant for GdIG and MF single phase is well matched with the literature. The lattice parameter of composites of GdIG increases slightly due to the effect of strain at the interface between GdIG and MF [36]. The modification that came due to the strain effect at the interface of composites also brings changes in the physical properties of composites. The variation in lattice constant is also because of dissimilarity in reciprocal solubility of

soft ferrites phases [37]. The micro-strain of the GdIG and its composites is calculated using Eq. 4.

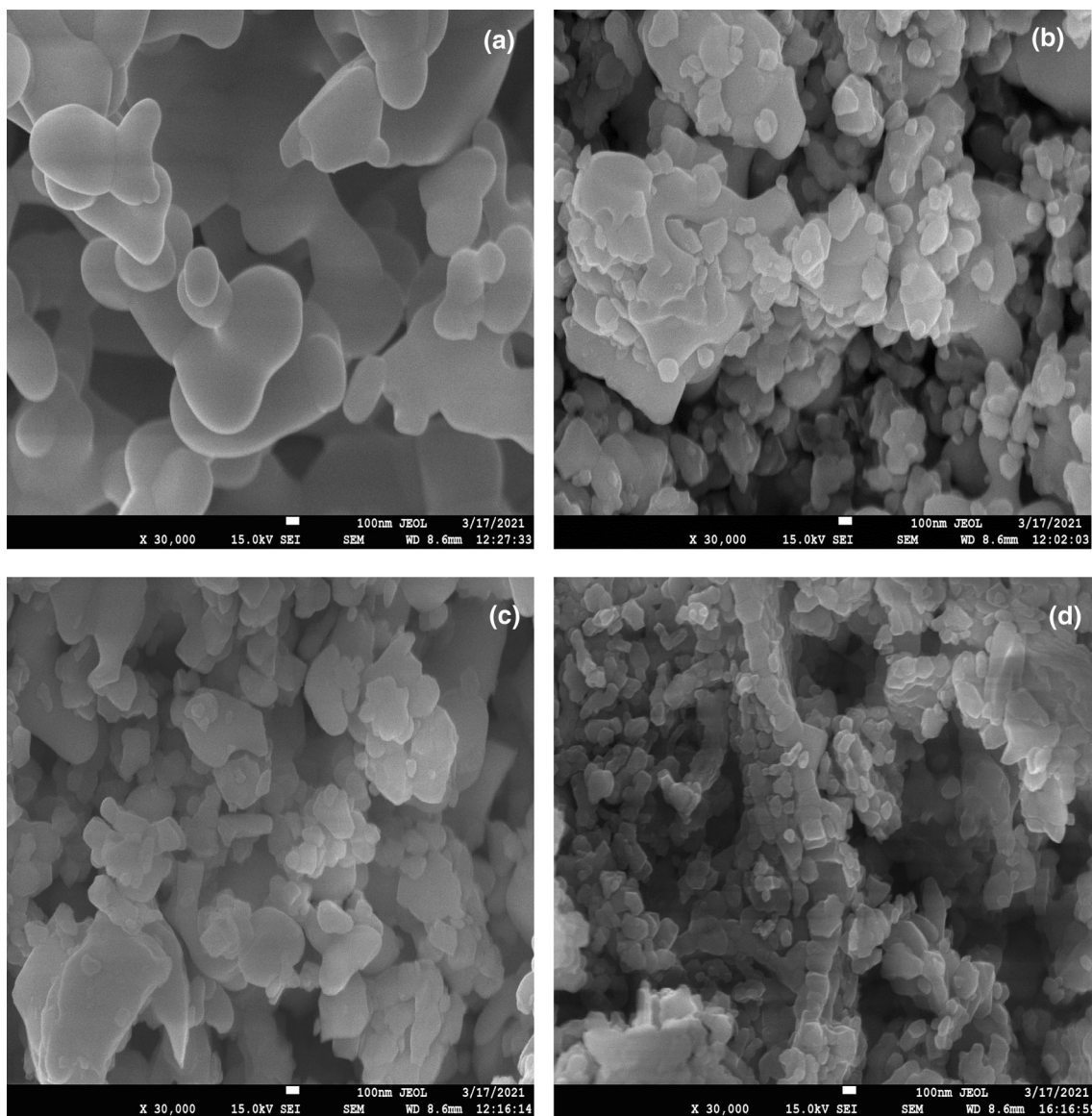
$$\varepsilon = \frac{\beta}{4 \tan \theta} \quad (4)$$

### 3.2. FESEM

Figure 3 shows the morphology of pure GdIG ( $x = 1.0$ ) and its composites. The micrograph (a) shows the presence of

**Table 1** Crystallite size, lattice parameter (a), and micro-strain calculated for GdIG and its composites

Composition Code	Garnet%-Spinel%	Crystallite Siz	Lattice Parameter(a)	Micro-Strain
x = 1.0	Garnet only (GdIG)	33.1 nm	12.45	0.5
x = 0.5	50%-50%	54.7 nm	12.48	2.28
x = 0.75	70%-25%	45.7 nm	12.50	2.25
MF	MgFeO	26.7 nm	8.37	

**Fig. 3** FESEM micrographs of (a) x = 1.0 (GdIG), (b) x = 0.5, (c) x = 0.75 and (d) MgFe<sub>2</sub>O<sub>4</sub>

the spherical structure of GdIG. The micrographs of GdIG composites (b) and (c) show the presence of agglomeration of grains. Micrograph (d) shows the presence of rough cube-shaped grains of MgFe<sub>2</sub>O<sub>4</sub> (MF). The agglomeration

increases with an increase in GdIG in the composites, i.e. at x = 0.75 (GdIG is 75% and MF is 25%), i.e. here agglomeration is more. This is related with magnetic attraction in nanoparticles, which is due to the contribution

of soft ferrite garnet [38–40]. The grains of spinel ferrite (MF) seemed to be distributed over the micrographs for both composites. The micrograph shows some big and small grains, which indicates the presence of both GdIG and MF in composites. The cube (MF grains) like grains seemed to be present on the surface of some spherical grains (GdIG grains). This implies that the grains of MF get absorbed on the surface of GdIG in their composites. This adsorption of spinel ferrite (MF) on garnet ferrite (GdIG) is because of similarity in the structure [41].

Figure 4 represents the Gaussian distributed histogram which tells about the size distribution of the GdIG and its composites. The obtained particle size is  $0.4\ \mu\text{m}$ ,  $0.42\ \mu\text{m}$ ,  $0.24\ \mu\text{m}$  and  $123\ \text{nm}$  for  $x = 1.0$ ,  $0.5$ ,  $0.75$  and  $\text{MgFe}_2\text{O}_4$  samples, respectively. The difference in particle size of composites is because of migration of grain boundaries between two phases having limited solubility [42]. It can be said that one ferrite affects the growth of other ferrite which further limits the grain boundaries motions.

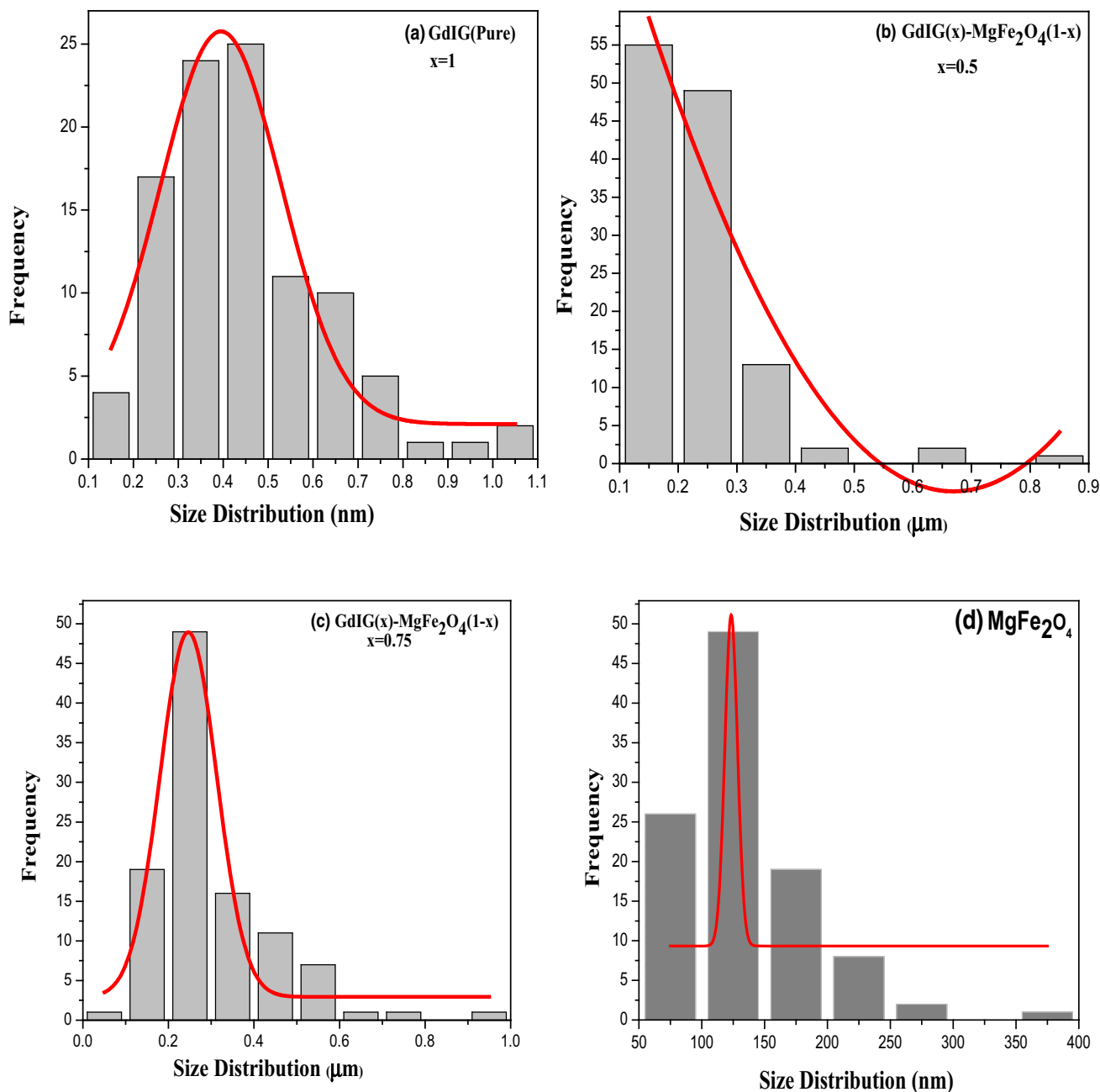


**Fig. 4** The Histograms representing size distribution of (a)  $x = 1.0$ , (b)  $x = 0.5$ , (c)  $x = 0.75$  and  $\text{MgFe}_2\text{O}_4$

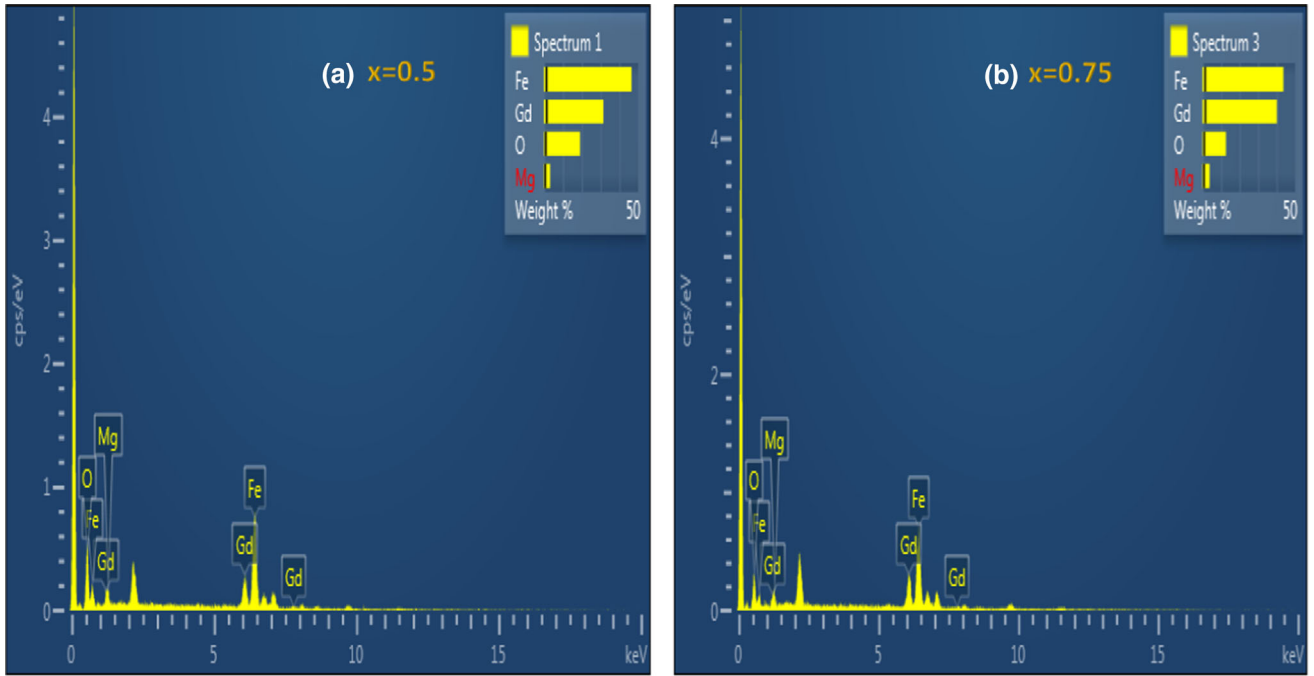


**Fig. 5** EDX spectra of composites (a)  $x = 0.5$  and (b)  $x = 0.75$

### 3.3. Energy dispersive X-Ray

The EDX spectra with chemical composition of the prepared composite are as shown in Fig. 5. It has been observed that the desired amount of the elements is present in the composites, with no extra sign of other elements. This implies that the synthesized method and temperature is efficient. It has been observed that with change in composition of composites, the change in chemical composition in EDX spectra is also observed.

### 3.4. Impedance analyser

The amount of resistance produced in presence of an electric field in a vacuum is known as permittivity. The complex permittivity ( $\epsilon^*$ ) has two parts, i.e. real ( $\epsilon'$ ) and imaginary ( $\epsilon''$ ) as given in Eq. (5) [40] and which are further related with impedance ( $Z^*$ ) as given in Eq. (6). The real part and imaginary part of complex permittivity can be calculated from impedance value and are given in Eqs. (7) and (8), respectively [43–49].

$$\epsilon^* = \epsilon' + \epsilon'' \quad (5)$$

$$\epsilon^* = \frac{1}{j\omega C_0 Z^*} \quad (6)$$

$$C_0 = \left( \frac{\epsilon_0 A}{t} \right)$$

Here,  $C_0$  is geometrical capacitance,  $\epsilon_0$  is the permittivity of free space having value  $8.85 \times 10^{-12}$  F/m,  $A$  is the area of

pellet, and  $t$  is the thickness of pellet measured using a vernier calliper.

$$\epsilon' = Z'' / 2\pi f C_0 (Z'^2 + Z''^2) \quad (7)$$

$$\epsilon'' = Z' / 2\pi f C_0 (Z'^2 + Z''^2) \quad (8)$$

Here,  $f$  is frequency,  $Z'$  and  $Z''$  are real and imaginary parts of the impedance, and these values are already given in the data of electrochemical spectroscopy.

The dielectric constant ( $\epsilon'$ ) versus frequency variation for the composites and GdIG and MgFe<sub>2</sub>O<sub>4</sub> is as shown in Fig. 6. Figure 6 has two parts (a) and (b) which represent the variation of  $\epsilon'$  at different frequency ranges. Figure 6 (a) represents the variation from 1 to 10 MHz ( $10^6$  to  $10^7$ ) range (higher frequency range) and (b) represents a variation from 1 Hz to 100 kHz ( $10^2$  to  $10^5$ ) range (lower frequency range). It is clear from the figure that the dielectric constant shows dispersion as the frequency changes. The dispersion of the dielectric curve can be explained using the theory given by Koop's [29, 51], which is based on the model of Maxwell–Wagner which explains about in-homogeneous double structure [52]. The structure of dielectric material was assumed to be formed by a double layer as stated by the model. Materials are well conducting in the first layer (grains), and materials are poor conductors in the second layer (grain boundaries). These layers are separated by each other. At higher frequency, grains of ferrites were effectual whereas, at a lower frequency, grain boundaries are more effectual. In garnet ferrites, only Fe<sup>+3</sup> ions are present, and in

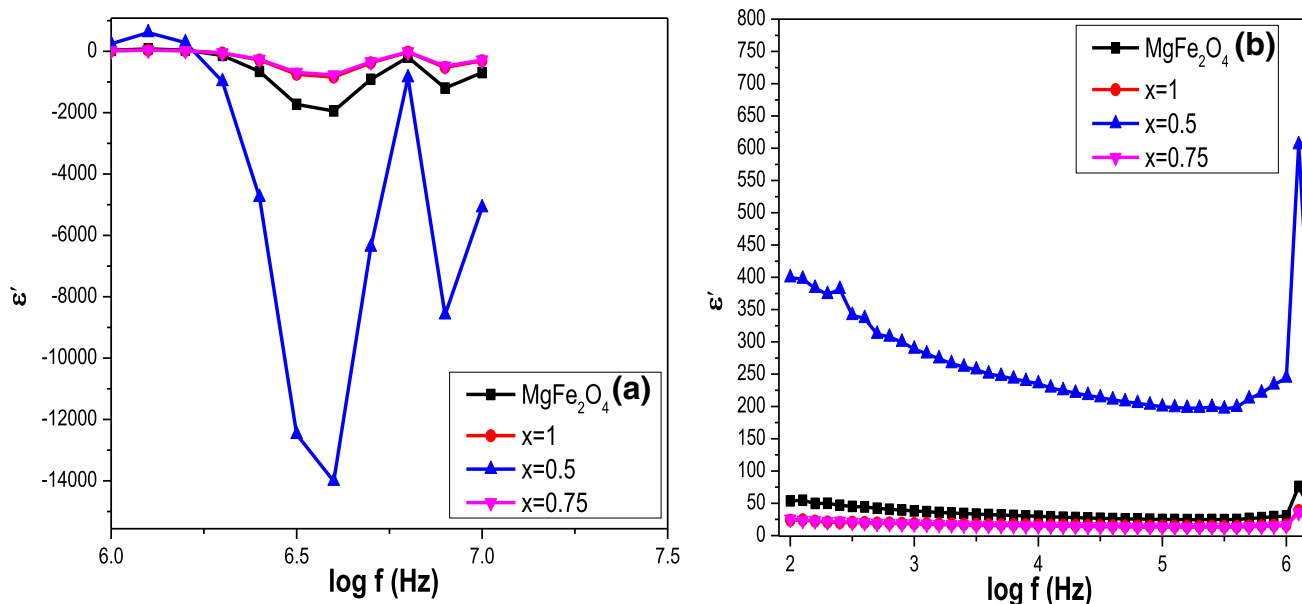


**Fig. 6** representing variation of dielectric constant ( $\epsilon'$ ) of  $\text{MgFe}_2\text{O}_4$  and  $x = 1.0, 0.5, 0.75$  at (a) 1 MHz to 10 MHz (b) 1 Hz to 100 kHz frequency

spinel ferrite, both  $\text{Fe}^{+3}$  and  $\text{Fe}^{+2}$  ions are present. This means that in composites,  $\text{Fe}^{+3}$  is dominant as compared to  $\text{Fe}^{+2}$ . These two ions offer dipolar to the ferrite's composites. The grains and grain boundaries are present in higher amounts in the ultrafine region as compared to the bulk, due to this, a complex phenomenon arises. Also, there is additional probability in nanomaterials to have a larger dielectric constant as individual grains have a larger surface area which further provides large polarization at the surface. The dielectric properties for ferrites can be more accurately determined by this surface polarization in a low-frequency region rather than ionic or electronic polarization [29].

It has been observed that GdIG ( $x = 1$ ) show almost constant value for  $\epsilon'$  from 1 Hz to 100 kHz (lower frequency region) shown in Fig. 6b which means it is showing frequency-independent behaviour whereas, in high frequency (Fig. 6a) region, its value varies slightly. By the addition of MF to GdIG, i.e. at  $x = 0.5$  gives the maximum value of  $\epsilon'$  near 1 MHz and there is a decrease in value of  $\epsilon'$  after this frequency range, i.e. up to 10 MHz. It shows more prominent decrease than  $x = 1$  and  $x = 0.75$ . Further at  $x = 0.75$ , i.e. on increasing GdIG ratio more, the values of  $\epsilon'$  show no variation with frequency from 1 Hz to 1 MHz. In the higher frequency region, it ( $x = 0.75$ ) follows the same trend as  $x = 1$ . It has been observed that a large value of dielectric constant  $\sim 612$  is obtained for  $x = 0.5$  at 1 MHz. It has been noticed that values of dielectric constant decrease by decreasing MF content (spinel ferrite) in GdIG, i.e. at  $x = 0.75$ , here the value of dielectric constant become almost independent of frequency up to 1 MHz such variations have also been

observed in pure GdIG. At a higher frequency, the value of the dielectric constant decreases which is a very obvious behaviour of ferromagnetic materials. In ferrites, the polarization mechanism can be understood similarly as conduction phenomena. As the  $\text{Fe}^{+3}$  ions and  $\text{Fe}^{+2}$  ions of composites exchange their electrons, the electron tends to displace in the direction of the field which is applied and hence polarization occurs. The decrease observed in the dielectric constant can be attributed to the fact that these charge carrying ions need some fixed time to align themselves in the direction of the applied AC field. The charges get disabled to align themselves in the applied field due to the high reversal frequency [53]. Here, the applied frequency increases continuously, and at some points, polarization has started to proceed so that no reverse field opposes their motion, but unable to provide any contribution to polarization and further there is no dielectric constant. So, in general, grain boundaries defect, oxygen vacancies, presence of  $\text{Fe}^{+2}$  enhances the dielectric constant at lower frequencies whereas when polarization and applied field lags out there is a decrease in dielectric constant at higher frequency [54].

The imaginary part ( $\epsilon''$ ) of dielectric constant for the composites, GdIG and  $\text{MgFe}_2\text{O}_4$  is as shown in Fig. 7. Further variation of  $\epsilon''$  is also measured in  $10^6$  to  $10^7$  and  $10^2$  to  $10^5$  range as given in (a) and (b) of Fig. 7. It can be seen that in lower frequency range GdIG ( $x = 1$ ),  $x = 0.5$ ,  $x = 0.75$  shows no variation in  $\epsilon''$ . This implies that GdIG and its composites are independent of frequency in a lower frequency range, whereas with the addition of MF in GdIG, i.e. at  $x = 0.5$ , the value of  $\epsilon''$  decreases near 1 MHz and



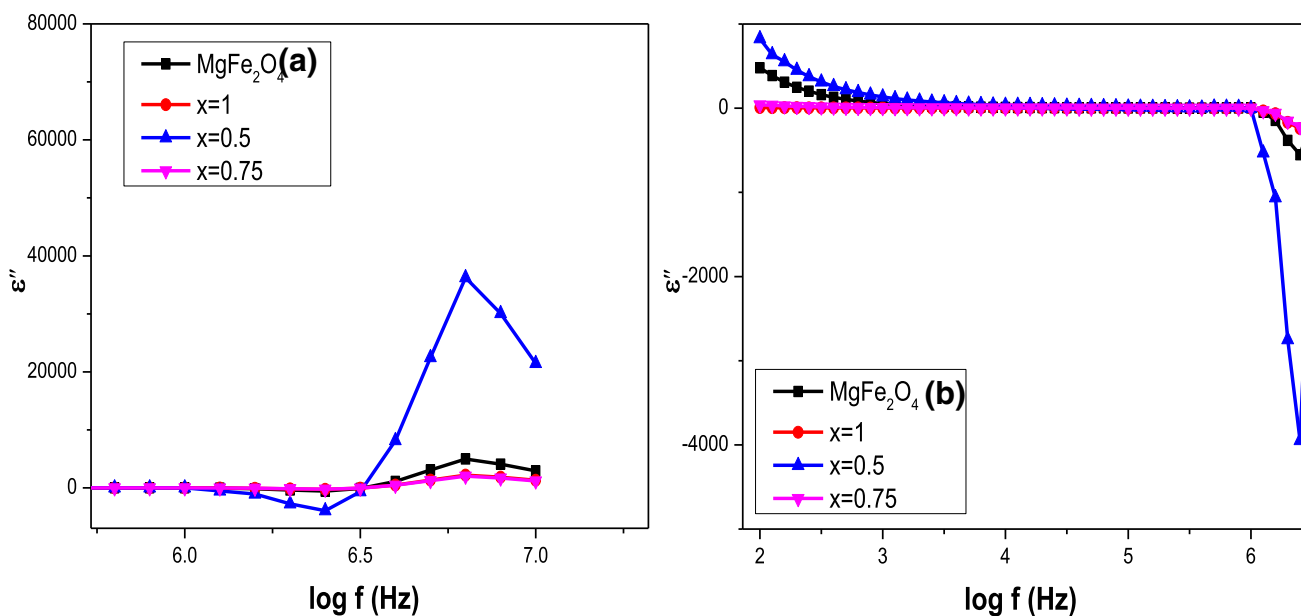


Fig. 7 represent variation imaginary part ( $\epsilon''$ ) of dielectric constant with frequency for  $MgFe_2O_4$  and  $x = 1.0, 0.5, 0.7$  at (a) 1 MHz to 10 MHz (b) 1 Hz to 100 kHz frequency range

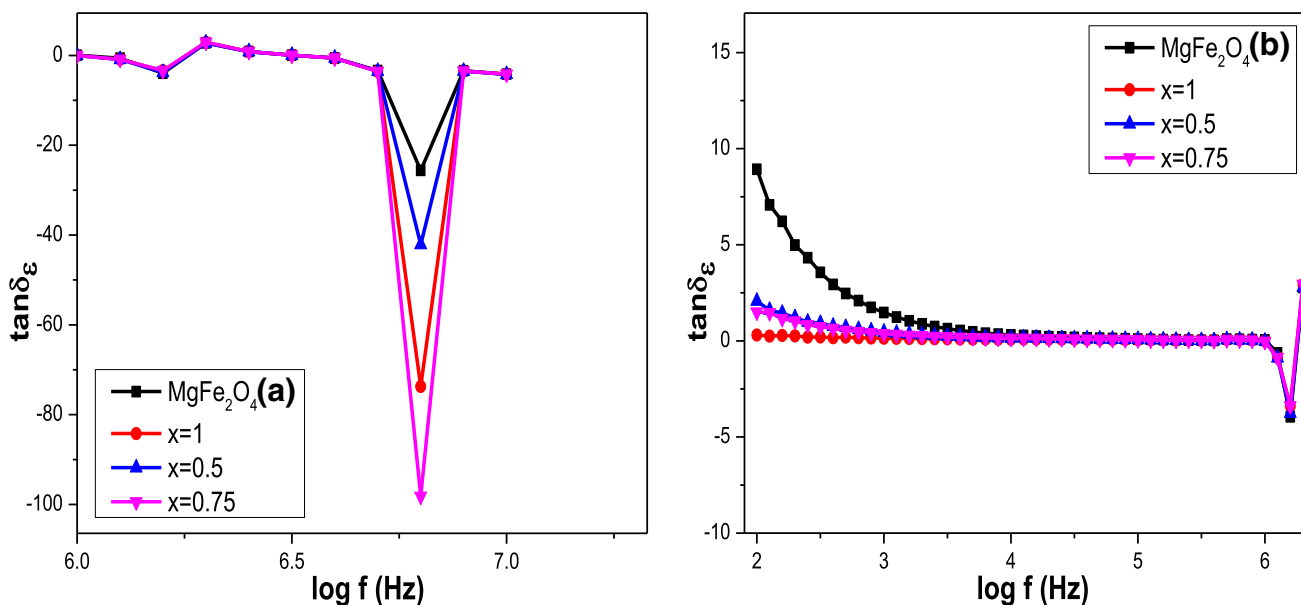


Fig. 8 The variation of dielectric tangent loss with frequency for  $MgFe_2O_4$  and  $x = 1.0, 0.5, 0.75$  at (a) 1 MHz to 10 MHz (b) 1 Hz to 100 kHz

then increases near 7 MHz. The value of  $\epsilon''$  is maximum for  $x = 0.5$  near about 7 MHz.

The dielectric tangent loss of samples is as shown in Fig. 8 and is calculated using Eq. 9 [55]. Dielectric loss is simply the loss of the energy induced by the applied field. It has been observed that for all composites, the losses are almost zero in the high-frequency region (up to 5 MHz) and not getting affected by frequency. But near 6 MHz, variations in losses are there. The value of loss tangent is least for  $x = 0.75$  composite and become maximum for

$x = 0.5$  composite at this frequency range. Whereas in the low-frequency region as shown in Fig. 8 (b),  $x = 0.75$  composite has a larger value of dielectric loss tangent nearly at 1 Hz frequency which further decreases with an increase in frequency. For  $x = 1$ , no such variation in the value of dielectric loss in the lower frequency region is there. The dielectric loss is caused by the resonance obtained at the walls of the domains. And also, when charge carries transport from grain-grain boundaries of ferrites and direction of polarization changes in presence of

applied field which cause dissipation in energy [56]. These domain wall motions are restricted at the higher frequency where magnetization causes the change in rotation so the losses are low at higher frequencies [57].

$$\tan \delta_e = \frac{\epsilon''}{\epsilon'} \quad (9)$$

### 3.5. VSM

Figure 9 represents the magnetization vs applied field curve (M-H) of MgFe<sub>2</sub>O<sub>4</sub> (MF), GdIG ( $x = 1$ ) and their composites ( $x = 0.5, 0.75$ ). The S-shaped curves signify the superparamagnetic nature of the samples. Single-phase magnetic nature has been observed by the addition of MF to GdIG. This suggests the exchange coupling between these two ferrites [29], which give rise to magnetization switching between the phases [42] of ferrites present in composites. The magnetic parameter coercivity ( $H_c$ ), retentivity ( $M_r$ ), saturation magnetization ( $M_s$ ), squareness ratio (SQR) is deduced from the M-H curve, and the value of anisotropy constant ( $K_{\text{eff}}$ ), magnetocrystalline anisotropy ( $H_a$ ), microwave operation frequency ( $\omega_m$ ) is tabulated in Table 2. The value of  $K_{\text{eff}}$ ,  $H_a$ , and  $\omega_m$  have been calculated using Eqs. (10), (11) and (12), respectively.

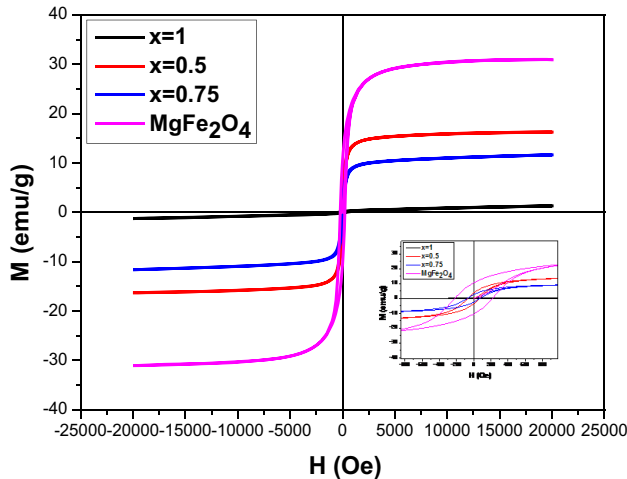


**Fig. 9** Magnetization hysteresis loops  $x = 1$ ,  $x = 0.5$ ,  $x = 0.75$  and MgFe<sub>2</sub>O<sub>4</sub> composites

$$K_{\text{eff}} = \frac{H_c \times M_s}{0.96} \quad (10)$$

$$H_a = \frac{2K_{\text{eff}}}{M_s} \quad (11)$$

$$\omega_m = 8\pi^2\gamma M_s \quad (12)$$

It has been observed that  $M_s$  value is least for  $x = 1$  (GdIG), maximum for  $x = 0.5$  (GdIG 50% and MF 50%) and moderate for  $x = 0.75$ . The larger value of  $M_s$  is attributed to the addition of MF in GdIG, which is due to disorder in spin, morphology at the surface and anti-phase disorder [40, 58]. The single-phase magnetization curve of ferrites is present despite two-phase nanocomposite which shows exchanged couple which is the reason for the enhancement in the value of  $M_s$ . If such behaviour of curve is not present, then there is superimposition between the two curves of ferrites, and at interphase, the spin arrangement is non collinearly, which tends to reduce the value of  $M_s$  [59].  $H_c$  is maximum for  $x = 1$ , and by the addition of soft ferrite (MF) in soft ferrite (GdIG) in nanocomposites, the value of  $H_c$  decreases for  $x = 0.5, 0.75$ . As by the addition of MF in GdIG, dipolar interaction becomes very important. Due to dipolar interaction, nucleation field reduces and further permits the reversal of domain in the soft ferrite phase in order to nucleate easily in presence of a low field so as a result of which value of  $H_c$  decreases [60–62]. The lower value of coercivity for composites signifies that the composites have soft nature. This means that composites easily get magnetized as compare to parent ferrites. While the trend observed of  $M_r$  can be understood by magneto crystalline anisotropy ( $H_a$ ) [63]. The value of  $H_a$  is larger for GdIG ( $x = 1$ ), which means it is very difficult to reverse magnetization by providing a low field. But by the addition of soft ferrite in GdIG, the value of  $H_a$  decreases. The ability of alignment of magnetization of ferrites in direction of applied field increases if dipolar interaction is more that it totally suppresses exchange-coupled interaction and hence  $M_r$  increases. The value of SQR for GdIG and its composites lies in the range 0.15 to 0.24 which is less than 0.5 signifies that all the samples have multi-magnetic domain structures. From the value of  $\omega_m$  (microwave operating frequency), it is clear that only

**Table 2**  $H_c$ ,  $M_r$ ,  $M_s$ , anisotropy constant, magnetocrystalline anisotropy, SQR and  $\omega_m$  calculated from MH for  $x = 0, 0.5, 0.75$  and MgFe<sub>2</sub>O<sub>4</sub>

Composition	$H_c$ (Oe)	$M_r$ (emu/g)	$M_s$ (emu/g)	M	$K_{\text{eff}}$ (erg/cm <sup>3</sup> )	$H_a$	SQR	$\omega_m$
$x = 1.0$	444.5	0.19	1.29	0.025	597.3	926	0.15	284 (MHz)
$x = 0.5$	65.4	3.82	16.2	0.325	1103.6	136	0.24	3.5 (GHz)
$x = 0.75$	73.7	2.68	11.63	0.233	892.8	153	0.23	2.5 (GHz)
MgFe <sub>2</sub> O <sub>4</sub>	220.2	10.5	31.04	0.6	7119	458	0.34	6.8 (GHz)

GdIG ( $x = 1$ ) can be operated in 284 MHz range but with the addition of MF into GdIG, this microwave operation frequency jumps into the GHz range, i.e. for  $x = 0.5$  nanocomposites can provide operation in 3.5 GHz range whereas for  $x = 0.75$  the range lies at 2.5 GHz. This implies that these nanocomposites can be operated at the S-band.

#### 4. Conclusions

The GdIG and MF were successfully prepared using the sol-gel auto-combustion method. GdIG composites ( $x = 1.0, 0.5, 0.75$ ) were prepared using mechanical blending according to wt.%. The XRD pattern shows the presence of a pure phase of GdIG and MF. It is found that for  $x = 0.5$  composite, both phases were present independently with sharper peaks, whereas at  $x = 0.75$  some GdIG peaks dominate. The crystallite size calculated from XRD data was found to be in the range 26–55 nm, which implies that samples are nanocrystalline. The average particle size obtained ranges from 0.24 to 0.42  $\mu\text{m}$  for  $x = 1, 0.5$  and 0.7. From the dielectric study, it has been observed that these composites show the variation of the real and imaginary part of the dielectric constant and loss tangent with frequency. Further from the M-H loop, it has been found that composites show better S-shaped curves as compared to GdIG which further tells about the superparamagnetic nature of composites. Value of  $M_s$  increases with increasing MF in GdIG,  $H_c$  decreases with the addition of MF in GdIG and  $M_r$  increases with the addition of MF. The calculated value of microwave operating frequency reveals that the addition of MF in GdIG enhances its operating frequency from MHz to GHz range which shows that alone GdIG is not sufficient to reach in GHz range its nanocomposites are the best option to operate in S-band.

#### Declarations

**Conflict of interest** The authors declare no conflict of interest.

#### References

- [1] A L Kozlovskiy *J. Ceram. Int.* **46** 8 10262 (2020)
- [2] M V Zdorvets and A L Kozlovskiy *J. Alloys comp.* **815** 152450 (2020)
- [3] N A Algarou, Y Slimani, M A Almessiere, S Güner, A Baykal, I Ercan and P Kögerler *Ceram. Intern.* **46** 7089 (2020)
- [4] K Seevakan, A Manikandan, P Devendran and Y Slimani *J. Magn. Mater.* **486** 165254 (2019)
- [5] K Pubby *J. Mater. Sci: Mater. in Elect.* **31** 599 (2020)
- [6] M N Akhtar, M A Khan, M Ahmad, M S Nazir, M Imran and A Ali *J. Magn. Mater.* **421** 260 (2017)
- [7] C P L Rubinger, D X Gouveia, J F Nunes, C C M Salgueiro, J A C Paiva and A M P F Grac *Technol. Lett.* **49** 1341 (2007)
- [8] D Ravinder *J. Mater. Sci. Lett.* **22** 1599 (2003)
- [9] W Chen, D Liu and W Wu *J. Magn. Magn. Mater.* **422** 49 (2017)
- [10] Z Jia and R D K Misra *Mater. Technol.* **26** 191 (2011)
- [11] B Seongatae *Nanotechnol.* **8** 86 (2009)
- [12] E S Lim and Y-M Kang *Mater. Today Commun.* **25** 1 (2020)
- [13] A A Novakova, V Y Lanchinskaya, A V Volkov, T S Gendler and T Y Kiseleva *J. Magn. Magn. Mater.* **258** 354 (2003)
- [14] C R Vesital and Z J Chang *Chem. Mater.* **14** 3817 (2002)
- [15] A A Sattar *J. Magn. Magn. Mater.* **412** 172 (2016)
- [16] T Arun, S Vairavel, S Gokul Raj and J Justin *Ceram Int.* **38** 2369 (2012)
- [17] E Garskaite, K Gibson, A Leleckaite, J Glaser and D Niznansky *J. Chem. Phys.* **323** 204 (2006)
- [18] M Yousaf, A Noor and S Xu *Cerm. Int.* **46** 16524 (2020)
- [19] K Praveena and S Srinath *J. Magn Magn. Mater.* **349** 45 (2014)
- [20] M N Akhtar, A B Sulong, S M Ahmad, M A Khan, A Ali and M U Islam *J Alloys and Compd.* **660** 486 (2016)
- [21] D-L Zhao *J. Alloys and Compd.* **480** 634 (2009)
- [22] R Pandey, L K Pradhan and M Kar *J. Phys. Chem. Soli.* 1 (2017)
- [23] V Skumryev, S Stoyanov, Y Zhang, G Handjipanayis, D Givord and J Nogués *Nature* **423** 850 (2003)
- [24] H Zeng, J Li, J P Liu, L Z Wang and S Sun *Nature* **420** 395 (2002)
- [25] M Pardavi-Horvath *J. Magn. Magn. Mater.* **215** 171 (2000)
- [26] C Sudakar *J. Magn. Magn. Mater.* **268** 75 (2004)
- [27] Z Zheng, H Zhang and J Q Xiao *J. Phys. D* **47** 115001 (2014)
- [28] C Pahwa and S Mahadevan *J. Alloys Compd.* **725** 1175 (2017)
- [29] R K Kotnala, S Ahmad and A S Ahmed *J. Appl. Phys.* **112** 054323 (2012)
- [30] M A Almessiere *J. Alloys Comp.* **767** 966 (2018)
- [31] A V Trukhanov et al. *RSC Advances* **10** 32638 (2020)
- [32] N A Algarou, Y Slimani, M A Almessiere and A Baykal *New Journal of Chemistry* **44** 5800 (2020)
- [33] M A Rahman *J. Magn. Magn. Mater.* **345** 89 (2013)
- [34] M George, A M John and S S Nair *J. Magn. Magn. Mater.* **302** 190 (2006)
- [35] M B Mohamed and K EL-Sayed *Composites: Part B* 1 (2013)
- [36] R Pandey, L K Pradhan and M Kar *J. Phys. Chem. Soli.* 1 (2017)
- [37] S Torkain *J. Magn. Magn. Mater.* **416** 408 (2016)
- [38] A Lopez-Ortega, M Estarder, G Salazar-Alvarez and A G Roca *J Nogués Phys. Rep.* **553** 1 (2015)
- [39] J Mohammed and H Y Hafeez *Res. Express* **6** 056111 (2019)
- [40] J Mohammed et al. *Chinese Phys. B* **27** 128104 (2018)
- [41] D Roy *J. Magn. Magn. Mater.* **321** L11 (2009)
- [42] B K Rai, L Wang and S R Mishra *J. Nanosci. Nanotechn.* **14** 5272 (2014)
- [43] Reetu, A Agarwal, S Sanghi, Ashima and N Ahlawat *J. Appl. Phys.* **113** 023908 (2013)
- [44] P G Fernandez and J A Aramburu *J. Phys. Chem. Lett.* **1** 647 (2010)
- [45] T Mizokawa *Rev. B* **60** 7309 (1999)
- [46] S Raghuvanshi and F Mazaleyrat *S N Kane AIP Adv.* **8** 047804 (2018)
- [47] J P Wright, A C McLaughlin and J P Attfield *J. Chem. Soc. Dalton Trans.* 3663 (2000)
- [48] M Guo, W Liu, X Xu, P Wu, H Zhang and Y Han *J. Nanoparticles Res.* **17** 460 (2015)
- [49] Md T Rahman, M Vargas and C V Ramana *J. Alloy. Compd.* **617** 547 (2014)
- [50] K Barick, K K Mishra and A K Arora *J. Phys. D Appl. Phys.* **44** 355402 (2011)
- [51] B K Bammannavar *J. Appl. Phys.* **104** 064123 (2008)
- [52] T Prodromakis and C Papavassiliou *Appl. Surf. Sci.* **255** 6989 (2009)

- [53] V R K Murthy and J Sobhanadari *Phys. Status Solidi A* **36** K133 (1976)
- [54] J C Maxwell (Oxford University Press, New York) p 828 (1973)
- [55] J Mohammed, T T Carol T, H Y Hafeez, D Basandrai, G R Bhadu, S K Godara, S B Narang and A K Srivastava *Results Phys.* **13** 102307 (2019)
- [56] N A Algarou et al. *J. Taiwan Inst. Chem. Eng.* **113** 344 (2020)
- [57] S Dagar and A Hoda *J. Alloys Compd.* **806** 737 (2019)
- [58] J E Davies, O Hellwiga, E E Fullerton, J S Jiang and S D Bader *Phys. Lett.* **86** 262503 (2005)
- [59] L Zhang and Z Li *J. Alloys Compd.* **469** 422 (2009)
- [60] N A Algarou et al. *A Manikandan and A Baykal Nanomaterials* **10** 1 (2020)
- [61] J P Liu *Nanoscale Magn. Mater. Applic.* 309 (2009)
- [62] C Rong, H Zhang and R Chen *J. Magn. Magn. Mater.* **320** 126 (2006)
- [63] H F Du and A Du *Phys. Stat. Solidi (b)* **244** 1401 (2007)

**Publisher's Note** Springer Nature remains neutral with regard to jurisdictional claims in published maps and institutional affiliations.